Indian Journal of Chemical Technology
Vol. 30, November 2023, pp. 746-752
DOI: 10.56042/ijct.v30i6.487

Mixed convection flow over non-Darcy porous stretching/shrinking sheet

Laltesh Kumar[1]*, Atar Singh[1], Kushal Sharma[2] & Vimal Kumar Joshi[3]

[1]Department of Mathematics, Agra College, Agra-282 004, Uttar Pradesh, India
[2]Department of Mathematics, MNIT Jaipur-302 017, Rajasthan, India
[3]Directorate of Online Education, Manipal University Jaipur-303 007, Rajasthan, India
*E-mail: lalteshjam@gmail.com

Received 12 April 2023; accepted 29 July 2023

An investigation has been carried out on heat and mass transport phenomena for mixed-convection flow over a vertically non-Darcy Forchheimer porous stretching/shrinking sheet considering the Soret - Dufour effects. With consideration of the appropriate similarity framework, the fundamental governing flow equations are converted into a system of non-dimensional equations. The bvp4c, a built-in solver of MATLAB software, is utilized to compute the numerical results of the flow problem. The present model is validated with previously published literature. The impacts of several related flow parameters on velocity, temperature, and concentration profiles have been displayed graphically. Also, the mass and heat transfer rates along with the coefficients of skin friction are calculated and discussed numerically. It is found that an increment in the thermal radiation parameter increases the fluid temperature, and the concentration gradient boosts up for the enhancement of the Soret number.

Keywords: Chemical reaction, Non-Darcy permeable medium, Soret-Dufour effects, Thermal radiation

Mixed convection flow on shrinking/stretching sheet is a phenomenon in which the buoyant motion acts perpendicular to the forced motion. The characteristics of heat transfer and double-diffusive flow with chemical reactions play a vital role in space technology, chemical industries, and hydrometallurgical industries etc. Because of this development, several books[1-2] presented theoretical work on mixed convective flow in the presence of porous media. In recent years, the transport phenomena because of mixed convection have been studied by many researchers. Sakiadis[3] investigated the behaviour of boundary layer flows on solid uniform flat surface which is finite in length using the integral method. He extended and broadened the shrinking sheet phenomenon by incorporating both the MHD fluid and mixed convection. The linearly stretchable boundary layer flow was first investigated by Crane[4]. Pal et al.[5] examined the transport phenomena influenced by chemical reaction on time dependent mixed convective fluid flow over a stretchable sheet saturated with non-Darcy porous channel. The heat transfer with chemical reaction in permeable medium has a vital role in moisture distribution over agricultural fields, crop damage from freezing, oxidation of solid materials.

For the high-speed flow, the non-Darcy model of convection across absorbent surfaces is highly trustworthy and becomes the center of attraction. The impact of melting in laminar flow and heat transfer in non-Darcy mixed steady flow was investigated by Hemalatha et al.[6]. Aghbari et al.[7] deliberated Buongiorno nanofluid model and 2-D mixed convection boundary layer flow in non-Darcy permeable medium in the occurrence of thermal diffusion. Sharma[8] investigated the effects of Darcy parameter and rotation on the magnetic nanofluid flow. In a porous medium, Ahmed et al.[9] discussed the flow with periodic permeability. Furthermore, in the same medium in a vertical plate, Bordoloi et al.[10] examined 3-D laminar flow in the occurrence of appreciable radiation with periodic suction and permeability.

A temperature gradient that results in a diffusion flux is what generates the Soret effect while the Dufour impact is a phenomenon of reciprocal heat-flux distinguished by a chemical potential gradient. In gases and liquids, both effects have undergone extensive research and become a fundamental problem. Joly et al.[11] examined buoyancy forces when natural convection flow occurs under the effect of Soret number in a vertical cavity. Bekezhanova et al.[12] studied two layers flows with diffuse evaporation in an infinite channel with the influence of the Dufour-Soret. Salleh et al.[13] discussed Buongiorno's nanofluid-model with the impact of Dufour-Soret on

forced convection flow for finding the stability of solutions by taking a very thin needle. The effects of thermal radiation with heat and mass transfer play a vital role when technological processes take place such as space technologies, missile re-entry rocket combustion chambers and the movement of pollutants from groundwater. Daniel et al.[14] examined the thermal behaviour of time-dependent and chemically reactive magnetohydrodynamic flow by considering the effect of thermal radiation and viscous dissipation. Mittal et al.[15] developed mathematical modeling on 2-D mixed MHD stagnation point flow with non-linear thermal radiation, chemical reaction, and for the impact of Brownian motion on the temperature gradient. Recently, many authors[16-17] explained the case of the inclusion of Dufour-Soret influences in the considered model for the flow study. In the recent past, Sharma et al.[18] discussed the effect of porosity with forced convective heat transfer on steady ferrohydrodynamic flow for water-based magnetic nanofluid over a rotating disk. Also, the significance of geothermal viscosity and thermal radiation for the magnetic fluid flow between co-rotating porous surfaces was discussed by Sharma et al.[19].

In the current study, the transport behaviour of mixed convective fluid flow on a vertically stretching/shrinking sheet in non-Darcy porous media is exhibited under the influence of the Soret-Dufour effects. The leading equations are renovated to PDE's to ODE's by using similarity variables. The numerical findings of the mathematical model are elaborated through graphs and tables. Here, the main objectives of the current study are:

- To study the consequences of chemical reaction on mixed-convection.
- How is liquid velocity influenced by non-Darcy porous media?
- How are temperature and concentration profiles influenced by cross-diffusion effects?

Experimental Section

Mathematical formulation of the problem

We assume 2-D laminar flow across an erect permeable sheet which is either shrinking or stretching in non-Darcy permeable, intermediate positioned in the plane $y = 0$. Consider velocity u along x-axis and velocity v along y-axis, where x and y components taking along the sheet and normal to the sheet (Fig. 1), respectively.

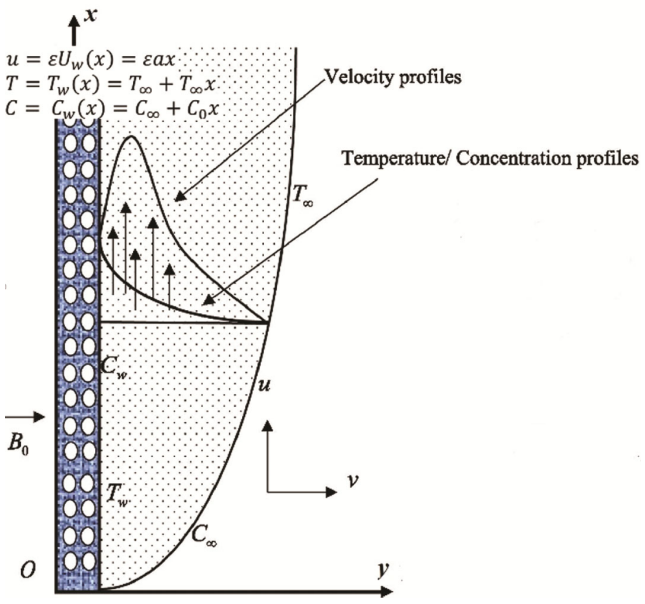

Fig. 1 — Schematic Diagram

The modeled system[5, 20] representing the problem is as follows:

Continuity equation:

$$\frac{\partial u}{\partial x} + \frac{\partial v}{\partial y} = 0. \quad \text{...(1)}$$

Momentum equation:

$$u\frac{\partial u}{\partial x} + v\frac{\partial u}{\partial y} = \nu\frac{\partial^2 u}{\partial y^2} + g\beta_T(T - T_\infty) + g\beta_C(C - C_\infty) - \rho\left(\frac{C_b}{\sqrt{k}}\right)u^2. \quad \text{...(2)}$$

Equation for fluid temperature:

$$u\frac{\partial T}{\partial x} + v\frac{\partial T}{\partial y} = \alpha\frac{\partial^2 T}{\partial y^2} - \frac{1}{\rho C_p}\frac{\partial q_r}{\partial y} + \frac{D_B k_T}{C_s C_p}\left(\frac{\partial^2 C}{\partial y^2}\right). \quad \text{...(3)}$$

Equation for mass concentration:

$$u\frac{\partial C}{\partial x} + v\frac{\partial C}{\partial y} = D_B\frac{\partial^2 C}{\partial y^2} - kr^*(C - C_\infty) + \frac{D_B k_T}{T_m}\left(\frac{\partial^2 T}{\partial y^2}\right). \quad \text{...(4)}$$

The boundary circumstances are,

$$\left.\begin{array}{c} u = \varepsilon U_w(x) = \varepsilon ax, v = \widehat{v_0}, \\ T = T_w(x) = T_\infty + T_\infty x,\ C = C_w(x) = C_\infty + C_0 x \ \text{ at } y = 0, \\ u = 0,\ T - T_\infty \to 0,\ C - C_\infty \to 0 \ as\ y \to \infty. \end{array}\right\} \quad \text{...(5)}$$

The thermal radiation is given by the Rossel and Approximation[21-24] and expressed as,

$$q_r = -\frac{4\sigma^*}{3k^*}\frac{\partial T^4}{\partial y}. \quad \text{... (6)}$$

Here $\sigma^*(= 5.67 \times 10 - 8\ \mathrm{W}/m^2k^4)$ is Stefan-Boltzmann constant, and mean-absorption constant is denoted by $k^*(m^{-1})$. By Taylor's expansion, we can expand T^4 as:

$$T^4 \cong -3T_\infty^4 + 4T_\infty^3 T \quad \text{...(7)}$$

Therefore, with the help of Eqs (6) and (7), the radiation effect is expressed as

$$\frac{\partial q_r}{\partial y} = \frac{-16\sigma^* T_\infty^3}{3kk^*}\frac{\partial^2 T}{\partial y^2} = -\frac{4}{3}Rd\frac{\partial^2 T}{\partial y^2}. \quad \ldots (8)$$

Here $Rd = \frac{4\sigma^* T_\infty^3}{kk^*}$ is the radiation parameter.

To non-dimensionalize the governing equations, the following transformations are used:

$$\frac{u}{ax} = f'(\eta), \quad \frac{v}{-\sqrt{a\nu}} = f(\eta), \qquad \theta(\eta) = \frac{T - T_\infty}{T_w - T_\infty},$$
$$\emptyset(\eta) = \frac{C - C_\infty}{C_w - C_\infty}, \qquad \eta = y\sqrt{\frac{a}{\nu}}.$$

Therefore, the Eqs (2) - (5) are transformed into non-dimensional equations as

$$\frac{d^3 f}{d\eta^3} + f\frac{d^2 f}{d\eta^2} - \left(\frac{df}{d\eta}\right)^2 + \lambda\theta + N\delta\phi - F_s\left(\frac{df}{d\eta}\right)^2 = 0. \quad \ldots(9)$$

$$\left(1 + \tfrac{4}{3}Rd\right)\frac{d^2\theta}{d\eta^2} + Pr\left(f\frac{d\theta}{d\eta} - \frac{df}{d\eta}\theta + Du\frac{d^2\emptyset}{d\eta^2}\right) = 0. \quad \ldots(10)$$

$$\frac{d^2\emptyset}{d\eta^2} + Le\left(-\frac{df}{d\eta}\emptyset + f\frac{d\emptyset}{d\eta} + Sr\frac{d^2\theta}{d\eta^2} - k_c\emptyset\right) = 0. \quad \ldots(11)$$

Subject to

$$f(0) = s, f'(0) = \varepsilon, \theta(0) = 1, \emptyset(0) = 1,$$
$$f'(\eta) \to 0, \theta(\eta) \to 0, \emptyset(\eta) \to 0 \ \ as\ \eta \to \infty. \quad \ldots (12)$$

Here, non-dimensionalised quantities are as follows:

$$Pr = \frac{\nu}{\alpha}, \qquad N = \frac{\beta_C C_O}{\beta_T T_O}, \qquad \delta = \frac{Gc}{Re_x^2}, Re_x = \frac{ax}{\nu},$$
$$Le = \frac{\nu}{D_B}, \qquad F_s = \frac{C_b x}{\sqrt{k}}, \qquad k_c = \frac{kr^*}{a}, \ \lambda = \frac{Gr}{Re_x^2},$$
$$Du = \frac{D_B k_T (C_w - C_\infty)}{C_s C_p \nu (T_w - T_\infty)},$$
$$Sr = \frac{D_B k_T (T_w - T_\infty)}{T_m \nu (C_w - C_\infty)}, \qquad Gr = \frac{g\beta_T (T_w - T_\infty)x^3}{\nu^2},$$
$$Gc = \frac{g\beta_c (C_w - C_\infty)x^3}{\nu^2}, \qquad Rd = \frac{4\sigma^* T_\infty^3}{kk^*}..$$

Also, we calculated the skin-friction coefficient, Nusselt and Sherwood numbers for the physical importance of the study.

$$\left.\begin{aligned} \tau_w &= \mu\left(\frac{\partial u}{\partial y}\right)_{y=0} \\ q_w &= -k\left(\frac{\partial T}{\partial y}\right)_{y=0} + (q_r)_{y=0} \\ q_m &= -D_B\left(\frac{\partial C}{\partial y}\right)_{y=0} \end{aligned}\right\}. \quad \ldots (13)$$

Now, the expression for τ_w(skin friction), q_w(heat exchange rate) and q_m(mass flux or rate of mass exchange) are taken as:

$$\left.\begin{aligned} (Re_x)^{\frac{1}{2}} C_f &= f''(0) \\ (Re_x)^{-\frac{1}{2}} Nu_x &= -\left(1 + \tfrac{4}{3}Rd\right)\theta'(0) \\ (Re_x)^{-\frac{1}{2}} Sh_x &= -\emptyset'(0) \end{aligned}\right\} \quad \ldots(14)$$

where $C_f = \frac{\tau_w}{\rho U_w^2}$ is known as skin friction coefficient, $Nu_x = \frac{xq_w}{k(T_w - T_\infty)}$, is known as Local Nusselt number and $Sh_x = \frac{xq_m}{D_B(C_w - C_\infty)}$ is known as local Sherwood number.

Results and Discussion

In this study, the solutions are found for the Soret-Dufour impact on a vertical non-Darcy porous stretching and shrinking sheet under thermal radiation and the transport consequences on the mixed convective flow of chemically reacting fluid. The numerical solutions of transformed Eqs (9)-(11) under the boundary conditions (12) are obtained by applying bvp4c MATLAB solver in which the ODE solver 'ode45' is used. To implement the bvp4c coding, the governing system of PDEs is converted to ODEs via suitable similarity transformations. Afterwards, higher-order ODEs are converted to a set of first-order ones, and then, the Runge-Kutta fourth-order method is employed. After that, the shooting technique is used to guess the values of unknown boundary conditions with the desired degree of accuracy, viz 10^{-6}. For the graphical outcomes, parameters fixed are for $Pr = 0.71$, $Le = 0.5$, $Rd = 0.1$, $N = 1$, $Sr = 1$, $Du = 0.2$, $s = 2$, $\lambda = -0.1$, and $\epsilon = -0.1$ with shown variations as depicted in figures.

Moreover, to validate the accuracy of computational results of the present study, heat transfer rate values are compared with the previous results of Dzulkifli et al.[20] in Table 1 and 2. From these tables, it can be seen that results are in excellent agreement. Furthermore, the results are discussed numerically through the tables and discussed through graphs.

Variation of velocity profile

The variation in the boundary layer velocity profile due to stretching parameter and the thermal radiation are exhibited in Figs 2 & 3, respectively. Fig. 2 illustrates the effect on velocity profiles when the flow passes over a sheet which is stretching when $\varepsilon > 0$ and shrinking when$\varepsilon < 0$. From the figure, it is noted that stretching of the sheet accelerates to rise in

Table 1 — Values of $f''(0)$ and $-\theta'(0)$ compare with Dzulkifli et al.[20], when $\lambda = -0.1, 1, 10$ for $Pr = 1, Le = 1,\ Rd = 0, N = 0, Sr = 0, Du = 0, s = 0, \varepsilon = 1$

λ	Dzulkifli et al.[20]		Present Study	
	$f''(0)$	$-\theta'(0)$	$f''(0)$	$-\theta'(0)$
-0.1	-1.1000	1.0520	-1.0720	1.0550
1	-0.6592	1.1090	-0.6257	1.1130
10	2.2020	1.3650	2.2670	1.3710

Table 2 — Values of $f''(0)$, $-\theta'(0)$ and $-\phi'(0)$ compare with Dzulkifli et al.[20] when $\lambda = -0.1, 1, 10$ for $Pr = 0.71, Le = 0.5, Rd = 0.1, N = 0.5, Sr = 1, Du = 0.2, s = 2, \varepsilon = 1$

λ	Dzulkifli et al.[20]			Present Study		
	$f''(0)$	$-\theta'(0)$	$-\phi'(0)$	$f''(0)$	$-\theta'(0)$	$-\phi'(0)$
-0.1	-2.5220	1.6480	0.5918	-2.5020	1.6650	0.6285
1	-1.4540	1.7520	0.6296	-1.4460	1.7660	0.6641
10	4.6520	2.1410	0.8030	4.6650	2.1520	0.8312

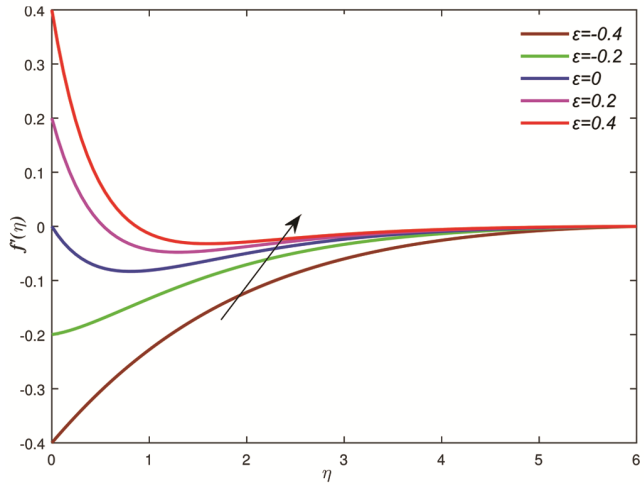

Fig. 2 — Plots of $\eta\ vs.\ f'(\eta)$ at different ε values

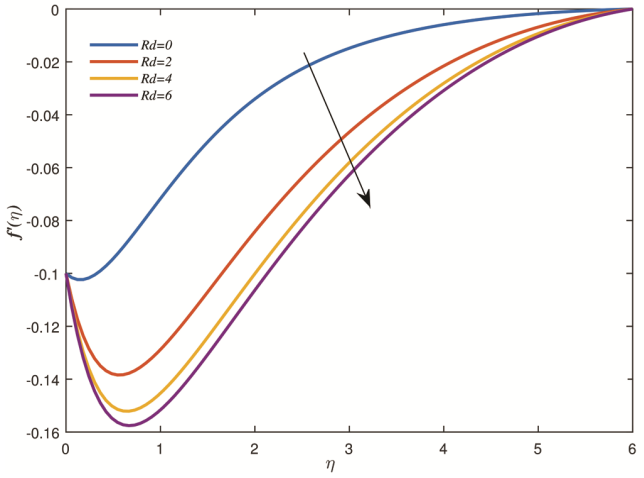

Fig. 3 — Plots of $\eta\ vs.\ f'(\eta)$ at different Rd values

the fluid velocity while the shrinking sheet diminishes the velocity. Fig. 3 shows how the radiation constraint (Rd) affects the velocity profiles of mixed convective fluid. It is observed that the velocity trend decreases

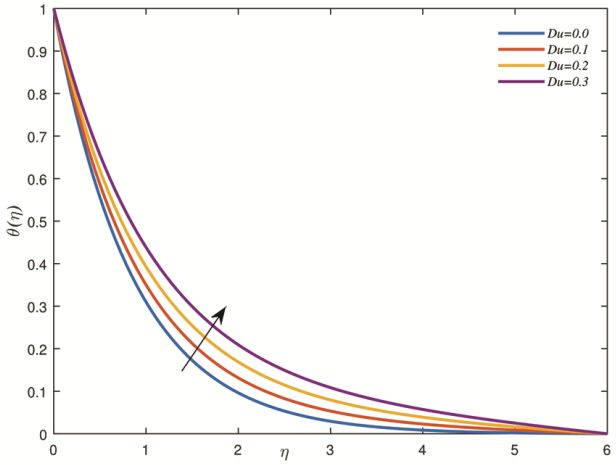

Fig. 4 — Plots of $\eta\ vs.\ \theta(\eta)$ at different Du values

on increasing the radiation parameter. In the absence of the radiation $(Rd = 0)$, the forward flow is observed when moving far from the sheet surface while the reverse flow is observed near the surface of the sheet for $0 < \eta < 1.0$ in the presence of the radiation.

Variation of Temperature Profile

Dufour effect reflects the amount of generated heat flux because of the concentration gradient. The role of the Dufour number on the temperature phenomenon is presented in Fig. 4. It is noted that the Dufour effect enhanced the boundary layer temperature of the fluid near the surface and therefore increasing Dufour number energized the boundary layer. The area below the temperature profile and the horizontal axis represents the thermal boundary layer thickness. Fig. 5 and Fig. 6 demonstrate the thicker thermal boundary layer thickness for the increasing value of the radiation parameter and thinner for increasing Prandtl number. The thermal boundary-layer

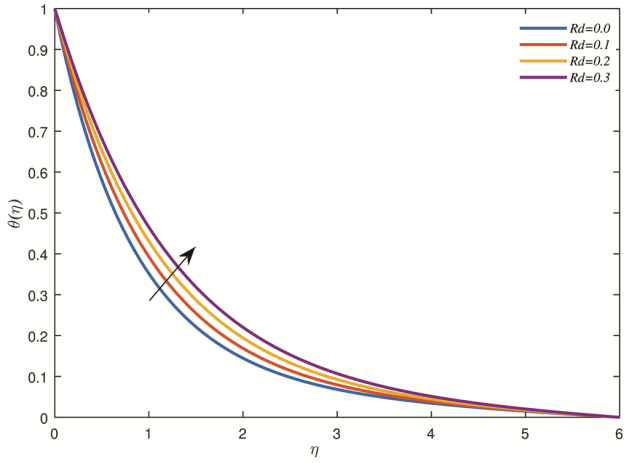

Fig. 5 — Plots of $\eta\ vs.\ \theta(\eta)$ at different Rd values

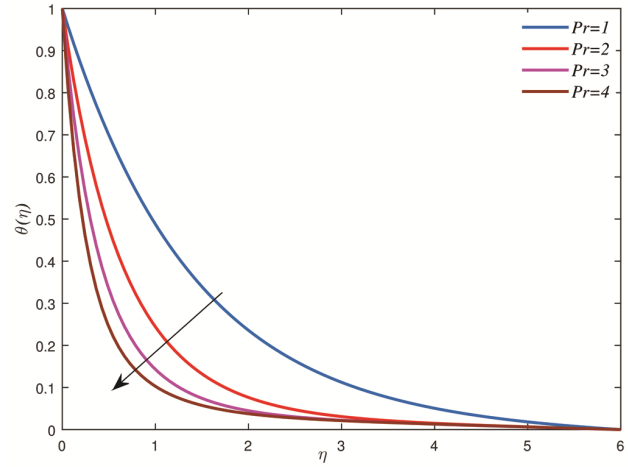

Fig. 6 — Plots of $\eta\ vs.\ \theta(\eta)$ at different Pr values

thickness is inversely proportional to heat dissipation. Therefore, the increase in radiation parameter refers to the slow and Prandtl number refers to the fast heat dissipation. Thus, increasing radiation causes the high temperature while increasing Prandtl number causes low temperature of the surface of the system.

Variation of concentration profile

The effect of the Soret parameter (Sr) (at $Du = 0.2$) on the concentration profile for the stretching state $(\varepsilon = 0.2)$ is shown in Fig. 7. It is seen that a surge in the Soret number uplifts the concentration as well as the boundary-layer thickness. Fig. 8 reveals that the increasing Dufour number (Du) enhances molar mass diffusiveness which encourages the mass concentration profile.The impact of Kc parameter on concentration profile is shown in Fig. 9. It is noted that near the surface $0 < \eta < 1.85$, the concentration of the flow reduces while for $1.85 < \eta < 6$, it enhances with the increase in the Dufour effect and converges to its steady state.

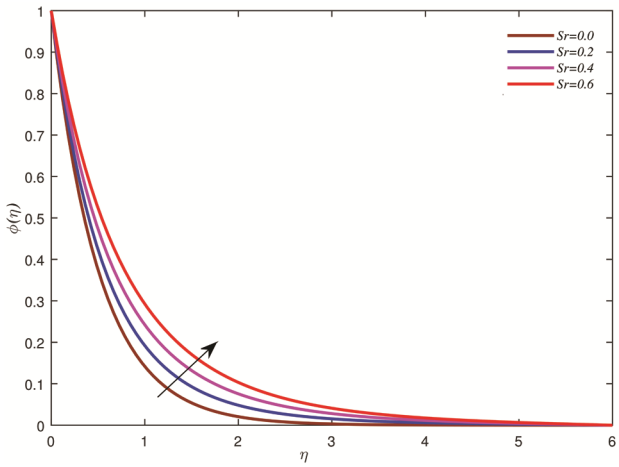

Fig. 7 — Plots of $\eta\ vs. \phi(\eta)$ at different Sr values

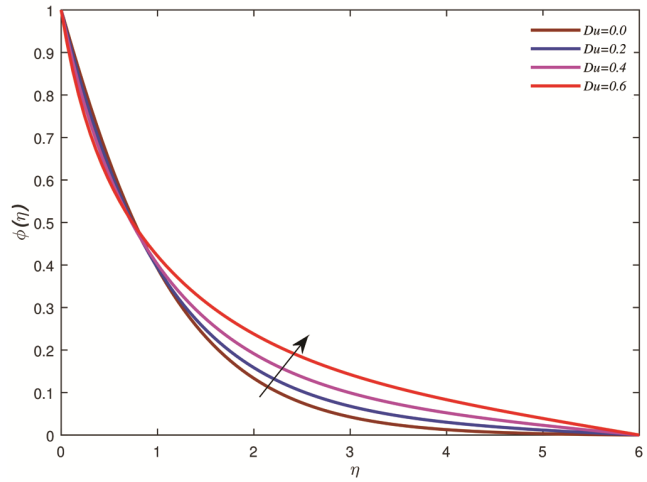

Fig. 8 — Plots of $\eta\ vs. \phi(\eta)$ at different Du values

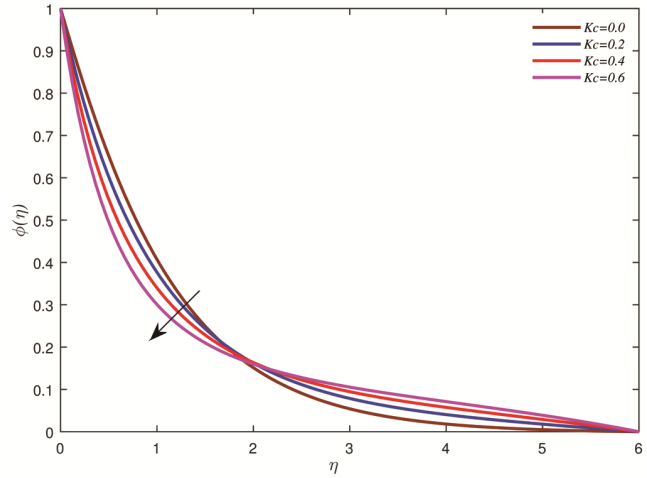

Fig. 9 — Plots of $\eta\ vs. \phi(\eta)$ at different Kc values

Further, the findings for skin-friction, Nusselt and Sherwood numbers have been discussed through Table 3. Here, it is observed that heat and mass transfer rates are enhanced with an increased Prandtl

Table 3 — Skin friction coefficient, Nusselt number and Sherwood number

Parameters	$-f''(0)$	$-\theta'(0)$	$-\emptyset'(0)$
Pr			
1.0	0.01077	01.56600	0.37840
2.0	0.02899	04.06200	-2.20000
4.0	0.00737	18.07000	-16.5700
Du			
0.0	0.008454	1.19300	0.80210
0.2	0.006327	1.04200	0.93090
0.6	0.044670	0.54190	1.35000
Sc			
1.0	0.006327	1.04200	0.93090
2.0	-0.032510	1.15900	2.13900
4.0	-0.060570	1.55900	6.38800
Kc			
0.0	0.00337	1.09300	0.80850
0.2	0.009517	0.99100	1.04800
0.6	0.02433	-0.78450	1.47400

and Schmidt numbers. In contrast, the opposite trend is observed for these parameters in the case of skin friction analysis. Likewise, Dufour number, thermal radiation parameter and chemical reaction parameters are observed to enhance the skin friction and rate of mass transfer; however, it is found to decelerate the heat transfer rate on the plate's surface for these parameters.

Conclusion

This study intends to investigate how mixed-convection, heat and mass transport through a vertical non-Darcy Forchheimer porous sheet (stretching/shrinking) are affected by chemical reaction and the Soret-Dufour effect. The imposing radiation leads to reversed decreasing flow near the surface of the sheet. Furthermore, boundary layer width is reduced in both circumstances of stretching and shrinking. There is a rise in fluid temperature profile for increasing values of radiation parameter. The enhanced Dufour effect and the Prandtl lead to reduce the heat flux, and thinner thermal boundary layer thickness which cause high heat dissipation and cooling of the sheet. The presence of Soret and Dufour effects lead to enhanced molar mass diffusiveness which enhances the mass concentration profile.

Nomenclature

(x, y)	Cartesian coordinates
(u, v)	Velocity coordinates along x-axis and y-axis (m/s)
β_c	Coefficient of solute expansion
$f(\eta)$	Dimensionless stream function
C	Concentration $(moles/Kg)$
β_T	Coefficient of thermal expansion $(1/K)$
σ^*	Stefan Boltzmann unvarying (W/m^2K^4)
D_B	Mass diffusivity parameter (m^2/s)
S	Dimensionless mass flux velocity
θ	Temperature parameter
$\emptyset$	Concentration parameter
A	Constant
F_s	Forchheimer Number
B_0	Magnetic flux density (T)
Gr	Grashof number for heat transfer
M	Magnetic parameter
T	Fluid temperature (K)
C_p	Specific heat at constant pressure (J/KgK)
C_∞	Concentration outside the boundary layer region $(moles/Kg)$
T_w	Stretching sheet parameter (K)
p	Pressure (Pa)
Pr	Prandtl number
α	Thermal diffusivity (m^2/s)
k_T	Thermal diffusion ratio $(K\ mole)$
C_s	Concentration susceptibility
Kr^*	Rate of Chemical reaction parameter
Sc	Schmidt number
Rd	Radiation parameter
k'	Roseland mean absorption
ε	Stretching/shrinking parameter
T_m	Mean temperature
q_r	Radiative heat flux
C_w	The species concentration at the plate surface
Du	Dufour number
Sr	Soret number
g	Acceleration due to gravity
Re_x	Local Reynolds number
Nu_x	Nusselt number
Sh_x	Sherwood number
Sc	Schmidt number
T_∞	Temperature outside the boundary layer region (K)
k^*	Mean thermal absorption coefficient
Cf_x	Skin friction coefficient
T_0	Temperature of the wall (K)
C_0	Concentration of the wall $(moles/Kg)$
N	Buoyancy ratio parameter
Le	Lewis number
δ	Density (Kg/m^3)
k_c	Chemical reaction parameter
G_c	Local concentration Grashof number
$f'(\eta)$	Velocity profile

Subscripts

w	Wall/surface
∞	Free stream

Superscripts

$'$	Derivative with respect to η

Greek Symbols

$\Psi(x, y)$	Stream function
k	Thermal conductivity (W/mK)
σ	Electrical conductivity $(1/ohm\ m)$
ρ	Density of the fluid (Kg/m^3)
η	Similarity variable
$\emptyset(\eta)$	Dimensionless concentration
μ	Dynamic viscosity of the fluid $(Pa.s)$

Re_x	Local Reynold's number
ν	Kinematic viscosity of fluid (m^2/s)
ψ	Stream function
λ	Mixed convection parameter

References

1 Schlichting H & Gersten K, *Boundary Layer Theory. Springer, New York* (2001).
2 Bejan A, *Convective Heat Transfer, 3rd Edn. Wiley, New York* (2013).
3 Sakiadis B C, *AIChE J*, 7 (1961) 26.
4 Crane L J, *J Appl Math Phys*, 21 (1970) 645.
5 Pal D & Mondal H, *Commun Nonlinear Sci Numer Simul*, 16 (2011)1942.
6 Hemalatha K, Kameswaran P K & Madhavi M V D N S, *Sadhana*, 40 (2015) 455.
7 Aghbari A, Agha H A & Sadaoui D, *J Mech*, 35 (2019) 851.
8 Sharma K, *Pramana J Phys*, 95 (2021) 113.
9 Ahmed N & Choudhury K, *Heat Transfer Asian Res*, 48 (2019) 644.
10 Bordoloi R & Ahmed N, *Biointerface Res Appl Chem*, 12 (2021) 7685.
11 Joly F, Vasseur P & Labrosse G, *Int Commun Heat Mass Tran*, 27 (2000) 755.
12 Bekezhanova V B & Goncharova O N, *Int J Heat Mass Tran*, 154 (2020) 119696.
13 Salleh S N A, Bachok N, Arifin N M & Ali F M, *Alex Eng J*, 59 (2020) 3897.
14 Daniel Y S, Aziz Z A, Ismail Z & Salah F, *J King Saud Univ Sci*, 31 (2019) 804.
15 Mittal A S & Patel H R, *Phys A: Stat Mech Appl*, 537 (2020) 122710.
16 Sharma K, Kumar S, Narwal A, Oudina F M & Animasaun I L, *Int J Appl Comput Math*, 8 (2022) 159.
17 Vijay N & Sharma K, *Multidiscip Model Mater Struct*, 19 (2023) 253.
18 Sharma K, Goyal R, Joshi V K, Bhardwaj S B, Singh R M & Makinde O D, *Indian J Eng Mater Sci*, 30 (2023) 283.
19 Sharma K, Vijay N, Ram D & Animasaun I L, *Numer Heat Transf A: Appl*, 84 (2023) 980.
20 Dzulkifli N F, Bachok N, Yacob N A, Arifin N Md, Rosali H & Pop I, *J Eng Math*, 132 (2022) 1.
21 Ram P, Singh H, Kumar R, Kumar V & Joshi V K, *Int J Appl Comput Math*, 3 (2017) 261.
22 Kumar S & Sharma K, *Chin J Phys*, 77 (2022) 861.
23 Sharma K, *Heat Transfer*, 51 (2022) 4377.
24 Sunil, Garg D, Joshi V K, Sharma K & Kumar S, *Pramana J Phys*, 97 (2023) 1.